



Discrete scaling based on operator theory

Aykut Koç^{a,b,*}, Burak Bartan^c, Haldun M. Ozaktas^a

^a Department of Electrical and Electronics Engineering, Bilkent University, Bilkent, Ankara, Turkey

^b National Magnetic Resonance Research Center (UMRAM), Bilkent University, Bilkent, Ankara, Turkey

^c Department of Electrical Engineering, Stanford University, Stanford, CA, USA

ARTICLE INFO

Article history:

Available online 4 November 2020

Keywords:

Discrete scaling

Scaling

Interpolation

Zooming

Operator theory

Hyperdifferential operators

ABSTRACT

Signal scaling is a fundamental operation of practical importance in which a signal is made wider or narrower along the coordinate direction(s). Scaling, also referred to as magnification or zooming, is complicated for signals of a discrete variable since it cannot be accomplished simply by moving the signal values to new coordinate points. Most practical approaches to discrete scaling involve interpolation. We propose a new approach based on hyperdifferential operator theory that does not involve conventional interpolation. This approach provides a self-consistent and pure definition of discrete scaling that is fully consistent with discrete Fourier transform theory. It can potentially be applied to other problems in signal theory and analysis such as transform designs. Apart from its theoretical elegance, it also provides a basis for numerical implementation.

© 2020 Elsevier Inc. All rights reserved.

1. Introduction

Signal scaling is a fundamental operation in which the independent variable of a function $f(u)$ is scaled by a real number M , resulting in the signal to be compressed or decompressed along the u axis in the form $f(u/M)$. With reference to images, the terms magnification/demagnification or zooming in/out are more commonly used. Unlike with signals of a continuous (real) variable, scaling or magnification is not straightforward for signals of a discrete (integer) variable: Given a function $f[n]$ defined on the integers, the value of $f[n/M]$ will be undefined unless n/M is an integer. Nevertheless, discrete scaling is a necessary operation in practice since we often want to scale signals which are represented as functions of discrete variables in digital computers.

An elementary approach [1–3] is to consider the values of $f[n]$ as the Nyquist-rate samples of a hypothetical bandlimited signal $f(u)$. Then, we can use standard sinc interpolation to write an expression for $f(u)$ in terms of $f[n]$. Now, $f(u)$ can be scaled to $f(u/M)$ and then re-sampled to obtain the values of a new signal of a discrete variable, which can be considered the scaled version of $f[n]$. The values of the new scaled signal will be linearly related to the values of the original signal $f[n]$. Of course, scaling $f(u)$ to obtain $f(u/M)$ will change its bandwidth, which necessitates care in choosing the re-sampling rate. If the re-sampling rate is different, this somewhat complicates interpretation of the scaled signal. If the integer domain is not defined from $-\infty$ to ∞ , but

rather over a finite interval, say from 0 to $N - 1$, and we are working in a circulant domain, it is possible to modify the approach by deploying Dirichlet functions [4] instead of sinc functions.

From a practical perspective (for instance, in image processing), discrete scaling is essentially a matter of interpolation, and has been addressed with a multitude of refined algorithms [5–8]. From a purer perspective, scaling is a basic operation in signals and systems theory, as well as optics and other forms of wave propagation [4,9,10]. For instance, the scaling operation is one of the special cases and building blocks of linear canonical transforms (LCTs) and widely used in its applications as well as in theoretical developments [11–20]. Our objective is not to propose new ad-hoc refinements to existing interpolation methods, but to propose a method for defining discrete scaling that is consistent with discrete Fourier transform (DFT) theory.

Given the purpose of the present paper, we limit ourselves to mentioning a few review articles from the vast literature on interpolation [5–8,21–23]. We will focus on a number of methods that can be used as standard baselines. We will use *nearest-neighbor*, *spline* and *linear interpolation* methods ([24–32]) as baselines for comparison. An approach that deviates from most others and which is more relevant to the present study is that by Pei et al., who developed a method based on “Centered Discrete Dilated Hermite Functions” (CDDHFs) [33], which is an improvement of their earlier “ n^2 matrix” method [34]. The CDDHF-based discrete scaling method works as follows: First, write the signal as a linear superposition of discrete Hermite-Gaussian functions. Then, replace the discrete Hermite-Gaussian functions with their dilated (scaled) versions to obtain the scaled discrete signal [33]. In other words,

* Corresponding author.

E-mail address: aykut.koc@bilkent.edu.tr (A. Koç).

the expansion coefficients are kept the same while scaling the discrete functions that form the expansion basis. Although this sounds conceptually simple, the difficulty (and ingenuity) lies in the development of the set of dilated discrete Hermite-Gaussian functions, [33,35], on which the method rests. This procedure provides a mathematically sound and elegant way of performing discrete signal scaling. Note that the method does not involve interpolation, which is why we give it special attention.

A different approach is presented in this paper, that utilizes hyperdifferential operator theory [4,13,36–41] to obtain a discrete scaling matrix. The scaled version of the signal is obtained by multiplying the unscaled version by this matrix. We choose to work in a framework that is not only discrete, but also finite. That is, the functions are defined over finite intervals. Our approach employs discrete versions of the basic operations of differentiation and coordinate multiplication. We believe that it provides a pure, elegant, and self-consistent definition of discrete scaling which is also fully compatible with DFT theory and its circulant structure. We also believe that the presented approach of defining a discrete operation in the context of hyperdifferential operator theory can set an example that can be applied to other problems in signal theory and analysis.

The paper is organized as follows: preliminaries are given in Section 2. In Section 3, we review Pei’s method. Our method is presented in Section 4. Numerical results and comparisons are given in Section 5. Finally, we conclude in Section 6.

2. Preliminaries

For simplicity we work with one-dimensional signals, although our results can easily be generalized to higher-dimensional signals (an image example is presented in Section 5). Scaling is defined as the operation which takes $f(u)$ to $|M|^{-1/2}f(u/M)$. The factor $|M|^{-1/2}$ is included to make the operation unitary, but this will not be of much importance. The real parameter $M > 0$ can be called the scaling or zooming factor or the magnification, depending on context. The signal will be compressed/demagnified or decompressed/magnified depending on whether M is less or greater than unity. In operator form we will write

$$\mathcal{M}_M f(u) = |M|^{-1/2} f(u/M), \quad (1)$$

where the calligraphic operator on the left-hand side includes the scaling parameter M as a subscript. Our convention for the Fourier transform operator will be

$$\mathcal{F}f(u) = \int_{-\infty}^{\infty} f(u)e^{-j2\pi u\mu} du. \quad (2)$$

We define two further operators, the coordinate multiplication operator \mathcal{U} and the differentiation operator \mathcal{D} :

$$\mathcal{U}f(u) = uf(u), \quad (3)$$

$$\mathcal{D}f(u) = \frac{1}{j2\pi} \frac{df(u)}{du}, \quad (4)$$

where $(j2\pi)^{-1}$ term is to ensure that the coordinate multiplication and differentiation operators are precise Fourier duals (the effect of one in either domain is its dual in the other domain). Then, one can mathematically express the precise Fourier duality as follows:

$$\mathcal{U} = \mathcal{F}\mathcal{D}\mathcal{F}^{-1}. \quad (5)$$

Basically, the above equation says that, instead of multiplying a function $f(u)$ with u , we can instead take its inverse Fourier transform, differentiate it with respect to the frequency variable, divide

by $i2\pi$, and take its Fourier transform, and we will get the same result.

Throughout this study, we work on finite-length signals. It could also be assumed that these discrete signals are defined on a circulant domain, without any consequential difference. The length of signal vectors are denoted by N and the samples are defined on the interval of integers $[-\frac{N}{2}, \frac{N}{2} - 1]$ or $[0, N - 1]$. The sampled signals can be represented by column vectors with N rows.

The matrix representing the Fourier transformation will be the unitary discrete Fourier transform (DFT) matrix \mathbf{F} , with appropriate shifting/circulation of its rows and columns such that it is consistent with the index ranges. The elements F_{mn} of this N -point unitary DFT matrix \mathbf{F} can be written in terms of $W_N = \exp(-j2\pi/N)$ as follows:

$$F_{mn} = \frac{1}{\sqrt{N}} W_N^{mn}, \quad (6)$$

where m and n run through the index range.

We work with dimensionless coordinates; that is, the unit of u is not seconds or meters, it is unitless. Say the function $\hat{f}(x)$ of a continuous variable x in seconds or meters has an approximate extent lying over the interval $[-\Delta x/2, \Delta x/2]$, meaning most of its energy is contained in this interval. Likewise, say its extent in the frequency domain lies over the interval $[-\Delta f/2, \Delta f/2]$, where f is the frequency variable in Hz or inverse meters. Then we can introduce a parameter s , such that $u = x/s$ is a dimensionless number and choose to work with the function $f(u) = \hat{f}(su)$ instead of $\hat{f}(x)$. If we choose $s = \sqrt{\Delta x/\Delta f}$, then the extent of both $f(u)$ and its Fourier transform will lie in the interval $[-\sqrt{\Delta x\Delta f}/2, \sqrt{\Delta x\Delta f}/2]$. According to the sampling theorem, if a signal is contained within such an interval, it can be sampled with a sampling interval of $1/\sqrt{\Delta x\Delta f}$. Thus there will be $N = \sqrt{\Delta x\Delta f} / (1/\sqrt{\Delta x\Delta f}) = \Delta x\Delta f$ samples in all. The quantity $\Delta x\Delta f$ is often referred to as the time-bandwidth or space-bandwidth product. Re-expressing in terms of the number of samples N , we would be sampling over the interval $[-\sqrt{N}/2, \sqrt{N}/2]$ with a sampling interval of $1/\sqrt{N}$ for a total of N samples.

We compare the proposed approach with some well-known interpolation methods. Specifically, we have picked three interpolation methods (linear, spline, and nearest neighbor interpolations). In Section 5, we present numerical results comparing the performances of these interpolation methods and our approach. These techniques have been around for a very long time and naturally the literature on them is vast. A sampling includes [24–32].

Linear interpolation fits a first-order polynomial (a line) between successive data points. Spline interpolation fits piece-wise spline polynomials between data points (cubic splines in our experiments). Nearest neighbor interpolation assigns the value of the nearest data point to each query point. In all three of these methods, when $M < 1$, we need to assign values to query points that are outside the domain of the signal (extrapolation). The way we have handled this in our implementation for the presented experiments is to use the same interpolation method for the points outside the domain. For instance, for nearest neighbor interpolation, all the points outside the domain are assigned the value of the signal at the closest end point.

3. Pei’s method

In [33], Pei et al. consider scaling a finite signal $f[n]$ of length N . They let $f_M[n]$ denote the scaled discrete signal, with M being the scaling factor. The signal $f[n]$ is expressed as a linear combination of N linearly independent ‘‘Centered Discrete Dilated Hermite Functions’’ (CDDHFs):

$$f[n] = \sum_{p=0}^{N-1} c_{p,1} H_{p,1}, \quad (7)$$

where the $H_{p,1}$ are the CDDHFs of length N , and the $c_{p,1}$ are the coefficients. The coefficients are simply given by $c_{p,1} = \langle f[n], H_{p,1} \rangle$. The second subscript "1" denotes the CDDHF with no scaling. $H_{p,M}$ denotes the p th CDDHF with a scaling factor of M . The idea of the method lies at scaling the basis signals $H_{p,1}$, and keeping the expansion coefficients the same. Thus the scaled signal f_M is:

$$f_M[n] = \sum_{p=0}^{N-1} c_{p,1} H_{p,M}, \quad (8)$$

where the $H_{p,M}$ are scaled versions of the $H_{p,1}$ with a scaling factor M . To find the scaled versions of the basis signals, Pei et al. uses the differential equation

$$M^2 \frac{d^2}{du^2} \psi_p \left(\frac{u}{M} \right) - 4\pi^2 \left(\frac{u}{M} \right)^2 \psi_p \left(\frac{u}{M} \right) = \lambda \psi_p \left(\frac{u}{M} \right) \quad (9)$$

satisfied by the scaled Hermite-Gaussian functions of a continuous variable, denoted by $\psi_p(u)$, that are given as follows, [4]:

$$\psi_p(u) = A_p H_p(\sqrt{2\pi}u) e^{-\pi u^2}, \quad A_p = \frac{2^{1/4}}{\sqrt{2^p p!}}, \quad (10)$$

where $H_p(u)$ denotes the Hermite polynomials.

Eq. (9) can be rewritten and rearranged in terms of the coordinate multiplication operator \mathcal{U} and the differentiation operator \mathcal{D} :

$$(M^4 \mathcal{D}^2 + \mathcal{U}^2) \psi_p \left(\frac{u}{M} \right) = -\frac{M^2}{4\pi^2} \lambda \psi_p \left(\frac{u}{M} \right). \quad (11)$$

The next step is to find the discrete counterpart of Eq. (11). This is done by replacing the calligraphic abstract operators by boldface matrix operators: $(M^4 \mathbf{D}^2 + \mathbf{U}^2)$. Then, it is possible to compute the CDDHFs $H_{p,M}$ as the eigenvectors of this matrix. Here \mathbf{U} and \mathbf{D} are matrices that are the finite discrete counterparts of the abstract operators \mathcal{U} and \mathcal{D} . So the remaining task before implementing the method is to determine what \mathbf{U} and \mathbf{D} should be. Pei et al. define the matrix \mathbf{U}^2 as follows:

$$\mathbf{U}_{mn}^2 = \begin{cases} (m - \frac{N-1}{2})^2 & \text{if } m = n, \\ 0 & \text{otherwise,} \end{cases} \quad (12)$$

where \mathbf{U}_{mn}^2 is the m th row, n th column entry of \mathbf{U}^2 , and $m, n = 0, 1, \dots, N-1$. Intuitively, this corresponds to multiplying every entry in a signal by the square of the corresponding index in a centered manner (hence the $-(N-1)/2$ term). (It will be interesting to contrast this with our development of the \mathbf{U} matrix later on. We do not take for granted that \mathbf{U} should be a simple reflection of the form of the continuous manifestation of the \mathcal{U} operator, and indeed show that for a formulation satisfying complete structural symmetry, it should be chosen differently.)

Once \mathbf{U}^2 is defined, we have $\mathbf{D}^2 = \mathbf{F} \mathbf{U}^2 \mathbf{F}^{-1}$ by using the duality relation given in Eq. (5). The matrix \mathbf{F} is the standard DFT matrix. Finally, for any scaling factor M , we can form $(M^4 \mathbf{D}^2 + \mathbf{U}^2)$, and find its eigenvectors $H_{p,M}$, after which we can easily complete the process. More on the implementation details of this approach can be found in [33].

4. Hyperdifferential operator based approach to discrete scaling

It is an established fact that the scaling operator \mathcal{M}_M can be expressed in hyperdifferential form in terms of the \mathcal{U} and \mathcal{D} operators [4,36,39,41]:

$$\mathcal{M}_M = \exp \left(-j2\pi \ln(M) \frac{\mathcal{U}\mathcal{D} + \mathcal{D}\mathcal{U}}{2} \right), \quad (13)$$

where M is the scaling parameter.

Hyperdifferential operators have been very recently introduced to the signal processing literature in defining discrete transforms [13,38]. In this paper, we show how hyperdifferential operators can be used to define discrete scaling. Our approach is based on requiring that all of our discrete definitions have the same relationships and operational properties as their abstract operator counterparts. Therefore, we will require the discrete manifestations of Eq. (5) and Eq. (13) to have the same structure, with matrix operators replacing the abstract operators. As a consequence, Eq. (5) will hold for finite difference and matrix versions of the \mathcal{D} and \mathcal{U} operators and the matrix operator counterpart of \mathcal{M}_M will be

$$\mathbf{M}_M = \exp \left(-j2\pi \ln(M) \frac{\mathbf{U}\mathbf{D} + \mathbf{D}\mathbf{U}}{2} \right). \quad (14)$$

Thus, a discrete-variable function can be scaled by writing it as a column vector and multiplying with the scaling matrix \mathbf{M}_M . In order to obtain the scaling matrix, we need the first-order coordinate multiplication and differentiation matrices \mathbf{U} and \mathbf{D} , and then compute the matrix exponential of the expression inside the parentheses. Therefore our first task is to determine the \mathbf{D} and \mathbf{U} matrices.

For discrete-variable signals, the counterpart of differentiation is to take finite differences:

$$\tilde{\mathcal{D}}_h f(u) = \frac{1}{j2\pi} \frac{f(u+h/2) - f(u-h/2)}{h}. \quad (15)$$

If we let $h \rightarrow 0$, then we have $\tilde{\mathcal{D}}_h \rightarrow \mathcal{D}$, since the right-hand side goes to $(j2\pi)^{-1} df(u)/du$. This justifies the interpretation of $\tilde{\mathcal{D}}_h$ as a finite-difference operator.

Another established result in operator theory is that $f(u+h) = \exp(j2\pi h\mathcal{D})f(u)$ [4,36]. This allows Eq. (15) to be expressed as:

$$\begin{aligned} \tilde{\mathcal{D}}_h &= \frac{1}{j2\pi} \frac{e^{j\pi h\mathcal{D}} - e^{-j\pi h\mathcal{D}}}{h} \\ &= \frac{1}{j2\pi} \frac{2j \sin(\pi h\mathcal{D})}{h} = \text{sinc}(h\mathcal{D}) \mathcal{D}. \end{aligned} \quad (16)$$

If we make $h \rightarrow 0$, it can again be shown that $\tilde{\mathcal{D}}_h \rightarrow \mathcal{D}$, confirming our earlier observation.

Now, we consider the definition of $\tilde{\mathcal{U}}_h$. What first comes to mind might be to define the discrete coordinate multiplication matrix as a diagonal matrix with the elements along the diagonal being given by the coordinate values, with due adjustment for centering and discreteness, much as in Eq. (12). Although this seems reasonable, after careful consideration, we decided that this is not necessarily the correct approach. In order to obtain the most consistent formulation possible, we must insist on maintaining the structural symmetry between \mathcal{U} and \mathcal{D} . To this end, we define $\tilde{\mathcal{U}}_h$ in such a way that it is related to \mathcal{U} , precisely the way $\tilde{\mathcal{D}}_h$ is related to \mathcal{D} :

$$\tilde{\mathcal{U}}_h = \text{sinc}(h\mathcal{U}) \mathcal{U}. \quad (17)$$

If $h \rightarrow 0$, then $\tilde{\mathcal{U}}_h \rightarrow \mathcal{U}$, as expected. Furthermore, when $\tilde{\mathcal{U}}_h$ is defined in this manner, we have the following duality expression (which is the same as Eq. (5) satisfied by \mathcal{U} and \mathcal{D}):

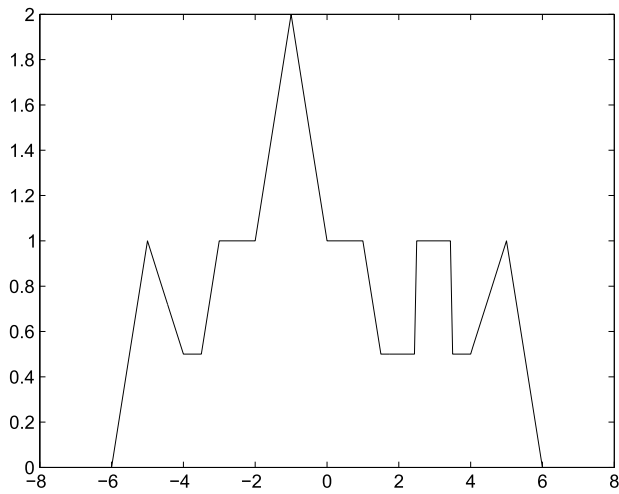


Fig. 1. Example signal F5.

Table 1
Percentage MSE scores for different methods with varying scaling factors M . Input Function: F1 (Chirped Pulse). $N = 512$.

M	Structural	Formal	Linear	Spline	Near Neig.	Pei's
0.33	0.0112	2.91e-19	4.04e-23	4.04e-23	4.04e-23	1.06
0.43	0.00369	2.43e-23	3.31e-4	6.1e-10	0.0958	0.472
0.52	0.00139	1.67e-23	3.04e-4	7.38e-10	0.17	0.219
0.62	5.57e-4	1.18e-23	3.39e-4	6.49e-10	0.116	0.101
0.71	2.16e-4	8.98e-24	3.38e-4	6.53e-10	0.111	0.0425
0.81	7.14e-5	6.46e-24	3.36e-4	6.45e-10	0.108	0.0147
0.90	1.41e-5	5.48e-24	3.17e-4	5.84e-10	0.11	0.00294
1.00	4.51e-24	4.51e-24	4.51e-24	4.51e-24	4.51e-24	5.21e-24
1.33	9.76e-5	2.65e-24	3.37e-4	6.53e-10	0.142	0.0166
1.67	3.44e-4	1.75e-24	3.37e-4	6.53e-10	0.111	0.0425
2.00	7.75e-4	1.1e-24	3.73e-4	8.39e-10	0.188	0.0664
2.33	0.00147	2.64e-24	3.37e-4	6.53e-10	0.115	0.0867
2.67	0.00253	1.69e-24	3.37e-4	6.53e-10	0.126	0.104
3.00	0.00406	6.76e-25	3.41e-4	6.11e-10	0.0964	0.118

Table 2
Percentage MSE scores for different methods with varying scaling factors M . Input Function: F2 (Trapezoid). $N = 512$.

M	Structural	Formal	Linear	Spline	Near Neig.	Pei's
0.33	0.0189	3.05e-4	2.24e-24	2.24e-24	2.23e-24	0.0573
0.43	0.0205	2.22e-4	8.17e-5	2.6e-5	0.00535	0.026
0.52	0.011	1.31e-4	3.9e-5	2.08e-5	0.00621	0.012
0.62	0.0107	4.01e-4	5.9e-4	2.55e-4	0.00643	0.00564
0.71	0.00502	8.94e-5	2.28e-4	6.72e-5	0.00589	0.00236
0.81	0.00332	4.57e-5	7.85e-5	2.28e-5	0.00666	8.32e-4
0.90	9.43e-4	5.4e-5	2.64e-5	4.11e-5	0.00654	1.83e-4
1.00	2.69e-25	2.69e-25	2.69e-25	2.69e-25	2.69e-25	3.26e-24
1.33	0.0118	7.85e-5	2.62e-4	9.27e-5	0.00764	9.75e-4
1.67	0.0498	5.31e-5	1.27e-4	5.08e-5	0.00607	0.00248
2.00	0.128	6.8e-5	2.14e-4	7.65e-5	0.0102	0.00391
2.33	0.26	6.81e-5	1.98e-4	7.51e-5	0.00629	0.00524
2.67	0.459	6.28e-5	1.97e-4	7.03e-5	0.00677	0.00668
3.00	0.734	8.78e-5	2.34e-4	9.79e-5	0.00528	0.00847

$$\tilde{\mathcal{U}}_h = \mathcal{F} \tilde{\mathcal{D}}_h \mathcal{F}^{-1} \tag{18}$$

This can be proved by substituting $\tilde{\mathcal{D}}_h$ in the above:

$$\begin{aligned} \tilde{\mathcal{U}}_h &= \mathcal{F} \left(\frac{1}{j2\pi} \frac{2j \sin(\pi h \mathcal{D})}{h} \right) \mathcal{F}^{-1} \\ &= \frac{1}{j2\pi} \frac{2j \sin(\pi h \mathcal{U})}{h} = \text{sinc}(h\mathcal{U})\mathcal{U}. \end{aligned} \tag{19}$$

The action of the operator \mathcal{U} on a continuous signal $f(u)$ is:

$$\tilde{\mathcal{U}}_h f(u) = \frac{1}{\pi} \frac{\sin(\pi hu)}{h} f(u). \tag{20}$$

Table 3
Percentage MSE scores for different methods with varying scaling factors M . Input Function: F3 (Damped Sine). $N = 512$.

M	Structural	Formal	Linear	Spline	Near Neig.	Pei's
0.33	0.65	0.0202	1.05e-12	5.07e-5	1.52e-17	18.6
0.43	0.244	0.00553	0.0468	1.67e-5	0.74	8.55
0.52	0.0849	0.00194	0.0203	3.47e-6	1.03	4.0
0.62	0.0335	7.73e-4	0.0419	6.54e-5	1.83	1.84
0.71	0.0127	3.13e-4	0.0398	1.08e-4	2.13	0.781
0.81	0.00406	1.12e-4	0.0475	8.38e-5	1.4	0.271
0.90	7.76e-4	2.49e-5	0.0316	2.89e-5	1.6	0.0543
1.00	8.48e-23	8.48e-23	8.48e-23	8.48e-23	8.48e-23	9.15e-23
1.33	0.00463	1.73e-4	0.0391	3.4e-4	2.34	0.306
1.67	0.0153	3.83e-4	0.0387	7.58e-4	1.92	0.783
2.00	0.0334	5.1e-4	0.043	9.56e-4	3.31	1.22
2.33	0.0621	5.53e-4	0.0387	9.94e-4	2.42	1.59
2.67	0.105	5.56e-4	0.0388	9.75e-4	2.07	1.9
3.00	0.165	5.53e-4	0.0392	9.57e-4	1.79	2.16

Table 4
Percentage MSE scores for different methods with varying scaling factors M . Input Function: F4 (Binary). $N = 512$.

M	Structural	Formal	Linear	Spline	Near Neig.	Pei's
0.33	19.2	3.47	0	2.12e-27	0	30.2
0.43	19.2	3.22	1.77	1.5	0	17.5
0.52	18.1	4.37	4.32	4.44	14.4	4.73
0.62	15.3	5.85	6.72	7.23	13.3	6.42
0.71	18.0	1.06	0.498	0.401	0	1.77
0.81	15.0	1.41	1.06	0.857	0	2.25
0.90	12.5	5.32	5.28	5.7	11.0	5.4
1.00	0	0	0	0	0	3.26e-24
1.33	24.9	5.57	5.17	5.62	9.07	4.55
1.67	37.3	3.52	3.45	3.53	8.12	3.94
2.00	40.9	29.2	2.75	2.75	5.5	16.2
2.33	38.8	238.0	3.44	3.56	9.98	110.0
2.67	156.0	542.0	4.27	4.5	10.5	241.0
3.00	379.0	776.0	4.95	5.3	10.8	428.0

Table 5
Percentage MSE scores for different methods with varying scaling factors M . Input Function: F5 (Medieval). $N = 512$.

M	Structural	Formal	Linear	Spline	Near Neig.	Pei's
0.33	2.17	0.246	4.14e-24	4.14e-24	4.12e-24	9.55
0.43	1.88	0.641	0.865	0.937	1.95	1.24
0.52	1.53	0.0555	3.7e-4	0.0246	0.0123	0.102
0.62	0.967	0.457	0.47	0.481	1.61	0.87
0.71	1.05	0.125	0.0602	0.0458	0.011	0.129
0.81	0.825	0.0812	0.0442	0.0362	0.0119	0.0926
0.90	0.804	0.309	0.299	0.274	0.0117	0.295
1.00	5.4e-25	5.4e-25	5.4e-25	5.4e-25	5.4e-25	4.33e-24
1.33	1.53	0.29	0.284	0.281	1.1	0.382
1.67	5.46	0.706	0.651	0.703	0.985	0.596
2.00	12.4	0.712	0.318	0.318	1.27	0.788
2.33	7.6	54.6	0.466	0.498	0.849	21.3
2.67	18.6	134.0	0.237	0.229	0.805	63.6
3.00	80.4	177.0	0.369	0.387	0.761	88.9

Note that the result is not simply multiplying the function with the coordinate variable. The alternative of defining $\tilde{\mathcal{U}}_h$ in a manner that corresponds to multiplying with the coordinate variable, destroys the symmetry and duality between \mathcal{U} and \mathcal{D} for discrete signals.

If we sample Eq. (20), the matrix operator that acts on discrete-variable signals can be obtained. The sampling points are chosen as $u = nh$ with n varying over a range that is determined by the number of sample N as explained in detail in Section 2. Finally, we are able to write the elements of the matrix \mathbf{U} :

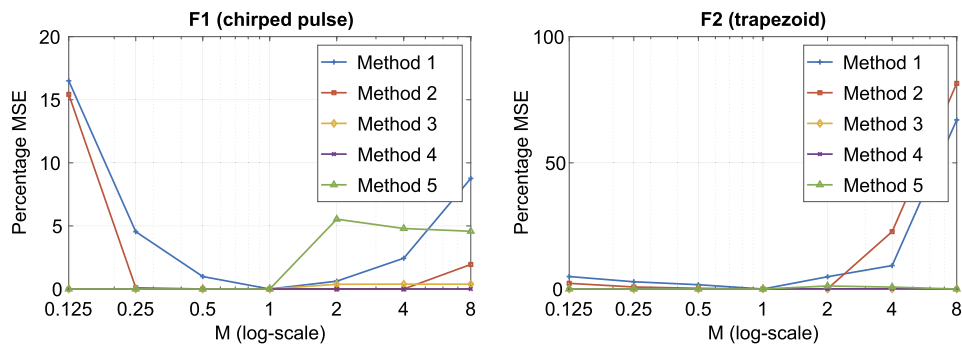


Fig. 2. MSE (%) as a function of M for functions F1 and F2.



Fig. 3. Barbara. $M = 0.6$. (From left to right; top to bottom: original, proposed (structural), proposed (formal), linear, spline, nearest).

$$U_{mn} = \begin{cases} (\sqrt{N}/\pi) \sin(\pi n/N), & \text{for } m = n, \\ 0, & \text{for } m \neq n. \end{cases} \quad (21)$$

$$\mathcal{D} = \mathcal{F}^{-1} \mathcal{U} \mathcal{F}. \quad (22)$$

Since we want the finite discrete manifestations of these abstract operators to also exhibit the same structure, we write

$$\mathbf{D} = \mathbf{F}^{-1} \mathbf{U} \mathbf{F}, \quad (23)$$

where \mathbf{F} was defined in Eq. (6). Thus, we have now obtained discrete matrix forms \mathbf{U} and \mathbf{D} of coordinate multiplication and dif-

We will refer to this definition as the *structurally analogous* definition of discrete coordinate multiplication.

The next step is to obtain the \mathbf{D} matrix. To do so, first recall that Eq. (5) can also be written as



Fig. 4. Barbara. $M = 1.6$. (From left to right; top to bottom: original, proposed (structural), proposed (formal), linear, spline, nearest).

ferentiation, and are finally in a position to calculate the discrete scaling operator defined in Eq. (14). We believe that the presented way of defining the finite matrix forms of coordinate multiplication and differentiation is the only way that is consistent with the dual nature of these operators, and the circulant structure of the DFT.

Before we move on to numerical results and interpretations, several comments will be in order. First of all, it will be worth recapitulating what we did and why. As mentioned, one approach is to define discrete coordinate multiplication by constructing a diagonal matrix with the elements given by the coordinate values. Then one can also easily obtain the discrete version of the differentiation matrix by using duality, without having to go through the circuitous route we followed. In other words, if \mathbf{U} is the coordinate multiplication operation, it can be discretized by a straightforward procedure: Assume N samples taken over an extent \sqrt{N} spaced $h = 1/\sqrt{N}$ apart. Then, we can discretize $\mathcal{U}f(u) = uf(u)$ as $nhf(nh) = n/\sqrt{N}f[n]$ with $u = nh$ and $n = 0, 1, \dots, N - 1$. Finally, \mathbf{U} can be expressed as

$$U_{mn} = \begin{cases} n/\sqrt{N}, & \text{for } m = n \\ 0, & \text{for } m \neq n \end{cases}, \quad (24)$$

where $m, n = 0, 1, \dots, N - 1$ or $n = -\frac{N}{2}, \dots, \frac{N}{2} - 1$. We will refer to this definition as the *formally analogous* definition of discrete coordinate multiplication. However, unlike Eq. (21), this definition is not consistent with the circulant structure of the finite/periodic lattice associated with the DFT.

Moving to another point, the simplest way to define the finite difference operator would have been, instead of Eq. (15),

$$\tilde{\mathcal{D}}_h f(u) = \frac{1}{j2\pi} \frac{f(u+h) - f(u)}{h}. \quad (25)$$

However, when discretized, the corresponding differentiation matrix would have values of -1 along the primary diagonal and values of 1 along the diagonal adjacent to the primary, leaving us with a matrix that is not symmetric. We rejected this option since the lack of symmetry does not allow to the elegant formulation obtained from Eq. (15). However, Eq. (15), while symmetric, did not allow us to immediately write a differentiation matrix, because it involved sample points in the middle of the sampling intervals, rather than the ends. Fortunately, the relationship Eq. (16) between $\tilde{\mathcal{D}}_h$ and \mathcal{D} that we derived showed the way to define $\tilde{\mathcal{U}}_h$. The operator $\tilde{\mathcal{U}}_h$ did not exhibit the same problem of involving sample points in the middle that $\tilde{\mathcal{D}}_h$ did, and could be discretized without



Fig. 5. Barbara. $M = 2.1$. (From left to right; top to bottom: original, proposed (structural), proposed (formal), linear, spline, nearest).

difficulty. It was also symmetrical, as desired. Once we obtained the \mathbf{U} matrix, it was possible to use duality to obtain the \mathbf{D} matrix as well.

To summarize, we defined two alternative operator theory based discrete coordinate multiplication operations. The first, given in Eq. (21), is structurally consistent with the DFT and theoretically desirable. The second one as given in Eq. (24), despite being based on the formal definition of the coordinate multiplication, lacks certain desirable properties. It will be seen, however, that despite its theoretical shortcomings, it has numerical advantages. We call the former “structural” and the latter “formal” definitions.

5. Quantitative discussion

In this section, we examine our formulation from a numerical perspective and then present computational cost analysis of our methods. We consider five different functions: a chirped pulse function $\exp(-\pi u^2 - j\pi u^2)$, denoted by F1, the trapezoidal function $1.5\text{tri}(u/2) - 0.5\text{tri}(2u)$ where $\text{tri}(u) = \text{rect}(u) * \text{rect}(u)$ denoted by F2, a damped sine function $\exp(-2|u|)\sin(2\pi 1.5u)$ denoted by F3, a binary sequence (01101010), denoted by F4, and the signal given in Fig. 1. We considered several different values for the scale parameter M , ranging from 0.33 to 3. To compute the

reference values, we used a computationally expensive, brute force numerical method and calculated normalized mean-square errors (MSE) between the following vectors: (i) Reference: Samples of the scaled functions $f(u/M)$ obtained by brute force; (ii) Discrete scaling: Samples obtained through our methods, Pei’s method and three baseline interpolation methods. In other words, we compare the following:

- Method 1: Proposed method I (Structural)
- Method 2: Proposed method II (Formal)
- Method 3: Linear interpolation
- Method 4: Spline interpolation
- Method 5: Nearest neighbor interpolation
- Method 6: Pei’s Method

The value of N , the number of samples, is taken as 512. Percentage MSE scores are tabulated in Tables 1 to 5 for a range of scaling factors M . Fig. 2 shows percentage MSE scores as a function of the scaling factor M for selected input functions.

Upon inspecting the results, one can make the following observations. First, our structurally analogous Method 1 outperforms Pei’s method in approximately two thirds of the input signal/scal-

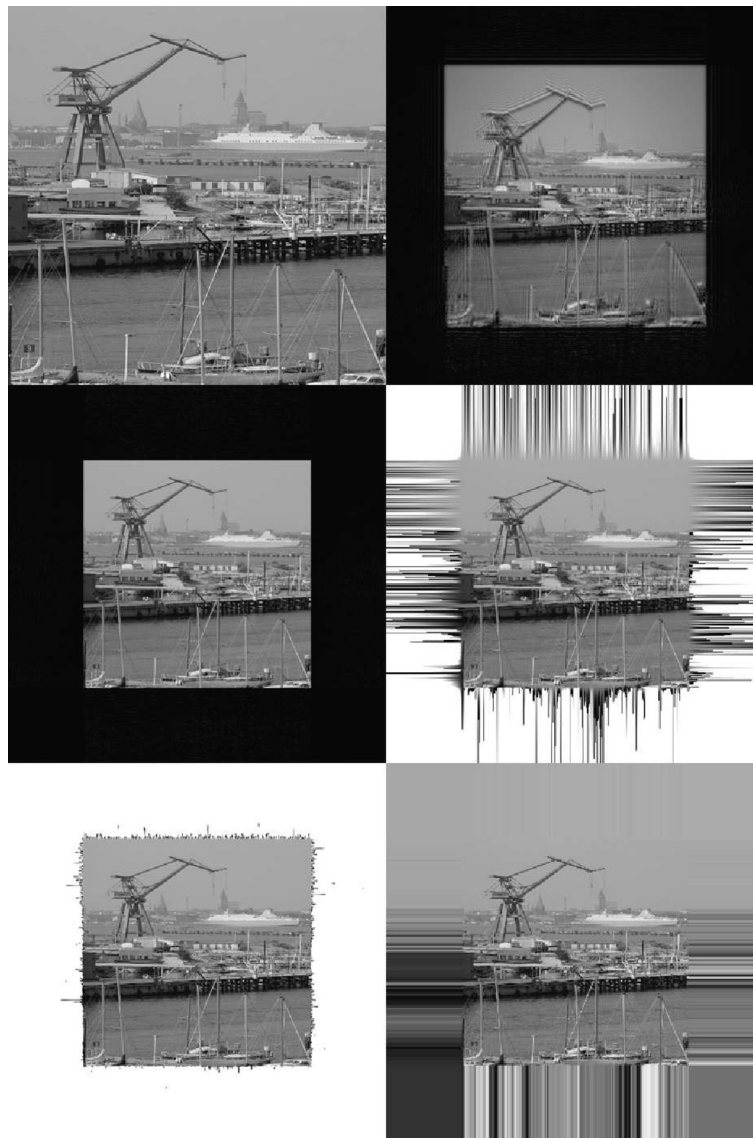


Fig. 6. Kiel Harbor. $M = 0.6$. (From left to right; top to bottom: original, proposed (structural), proposed (formal), linear, spline, nearest).

ing parameter pairs. On the other hand, our formally analogous Method 2 clearly outperforms Pei's method in all cases with great margins. Based on the numerical evidence, our proposed Method 2 clearly outperforms proposed Method 1 in terms of the MSE scores. Thus while Method 1 is the theoretically desirable alternative, Method 2 is to be preferred for practical numerical computation. Method 1 would have to be used with much higher values of N to achieve the same MSE as Method 2. The maintenance of strict structural analogy has a price in terms of numerical performance. Now we turn our attention to the comparisons with the three baseline interpolation approaches. Although the purpose of the present work is not to achieve ad-hoc numerical improvements to existing interpolation methods, Method 2 is also on par with all of the three baseline interpolation methods numerically.

We have also considered "Barbara" and "Kiel Harbor" images as 2D examples to make visual qualitative analysis. Results for different scaling parameters are given in Figs. 3 to 8. These images are also used in our experiments to verify the reversibility and additivity of our proposed method. Our discrete scaling framework is theoretically reversible and additive. This could be easily seen upon inspection of our definition given in Eq. (14). When one constructs two matrices by using Eq. (14) with scaling param-

eters M and $1/M$, these matrices are exactly inverses of each other. Theoretically, their successive application would be identity. However, in practical applications, for scaling values that correspond to zooming-in, some of the information in the original input can be lost. This, in turn, gives rise to some reconstruction errors in numerical simulations. We have presented sample results for reversibility experiments in Table 6 for "Barbara" and "Kiel Harbor" images and for several scaling parameters. The same theoretical considerations are also valid for additivity. Successive application of two scaling matrices that are obtained by Eq. (14) with parameters M_1 and M_2 to a signal would equal to application of a single matrix with parameter $M_3 = M_1 M_2$. Numerical examples for additivity experiments are presented in Table 7.

The results confirm that the presented approach to discrete scaling provides reasonable numerical performance, in addition to being attractive from a theoretical perspective. Higher accuracy (lower MSE) is obtained with increasing N . This is because large N means larger extents in both the time and frequency domains, so that a smaller percentage of the signal is left outside of these extents. As expected, the MSE values also depend on the signal that is being scaled. Recalling the considerations in Section 2, the accuracy obtained depends on what percentage of the signal energy is



Fig. 7. Kiel Harbor. $M = 1.6$. (From left to right; top to bottom: original, proposed (structural), proposed (formal), linear, spline, nearest).

confined within the chosen extents in the time and frequency domains. For example, MSE values for F2 are relatively higher than those for F1. This is caused by the fact that its frequency domain content is spread over a relatively greater extent, leading to a greater percentage of its energy to fall outside the chosen extents.

Comparison of the computational complexities of our approach and the other methods is as follows. The computational complexity for *generating* a scaling matrix of size $N \times N$ using our proposed methods is dominated by the computation of the matrix exponential. One way to perform matrix exponentiation is through computing the eigenvalue decomposition, which has complexity $O(N^3)$. Hence, in this case, generating the scaling matrix has complexity $O(N^3)$. Having said this, we note that if we precompute and store the scaling matrix for size N , then computing the scaled signal is of complexity $O(N^2)$ as we only need to do a matrix-vector product. Linear, spline, and nearest neighbor interpolation methods have computational complexity $O(N)$; however, their exact computational costs differ (hidden by the big-O notation). More precisely, nearest neighbor interpolation is the fastest one among these three methods and the second fastest one is linear interpolation. Pei's Method, similarly to our proposed methods,

involves computing the eigenvalue decomposition and has complexity $O(N^3)$.

6. Conclusion

We proposed a framework for scaling discrete-time signals based on hyperdifferential operator theory. We formulate a unitary scaling matrix that can be used to left-multiply vectors holding samples of finite-length signals of a discrete variable, to return the vector holding samples of the scaled version. The proposed formulation is mathematically elegant and pure in the sense that the structural relationships between all discrete entities completely mirror those between the continuous and abstract entities. Therefore, the structure obtained in the discrete world is strictly analogous to that in the continuous world. Furthermore, it also exhibits consistency with the circulant structure associated with the DFT. These theoretically attractive qualities do not result in the most accurate numerical method. However, the accuracy can be improved by maintaining the general hyperdifferential formulation, but only modifying the coordinate multiplication and differentiation matrices used. Thus although the purpose of this paper is not to provide numerical refinements, the result is numerically competitive. Al-



Fig. 8. Kiel Harbor. $M = 2.1$. (From left to right; top to bottom: original, proposed (structural), proposed (formal), linear, spline, nearest).

Table 6

Percentage MSE scores for reversibility with varying scaling factors M . Normalized by the energy of the input image.

M	$1/M$	Barbara		Kiel Harbor	
		Structural	Formal	Structural	Formal
0.5	2	1.094	1.976	2.209	2.844
0.6	1.667	0.728	1.332	1.714	2.111
0.7	1.429	0.456	0.781	1.253	1.518
0.8	1.25	0.252	0.172	0.859	0.937

ternative coordinate multiplication and differentiation matrices not considered in this paper can also be experimented with.

Finally, we also believe that the use of hyperdifferential operator theory to the problem of defining a discrete operation might open up new research directions for other applications in signal analysis and processing.

Declaration of competing interest

The authors declare that they have no known competing financial interests or personal relationships that could have appeared to influence the work reported in this paper.

Table 7

Percentage MSE scores for additivity with varying scaling factors M . Normalized by the energy of the output image obtained by direct scaling with parameter M_1M_2 .

M_1	M_2	M_1M_2	Barbara		Kiel Harbor	
			Structural	Formal	Structural	Formal
0.6	1.6	0.96	0.087	0.213	1.428	1.746
0.7	0.8	0.56	0.201	0.056	0.225	0.061
1.2	1.3	1.56	0.341	0.306	0.494	0.407
0.9	2.5	2.25	0.069	0.025	0.615	0.694

Acknowledgment

H.M. Ozaktas acknowledges partial support of the Turkish Academy of Sciences.

References

- [1] A.V. Oppenheim, A.S. Willsky, S.H. Nawab, Signals & Systems, 2nd ed., Prentice-Hall, Inc., Upper Saddle River, NJ, USA, 1996.
- [2] A.V. Oppenheim, R.W. Schaffer, Digital Signal Processing, Prentice-Hall, Inc., 1975.
- [3] A.V. Oppenheim, R.W. Schaffer, Discrete-time Signal Processing, 3rd ed., Pearson Education Limited, 2013.

- [4] H.M. Ozaktas, Z. Zalevsky, M.A. Kutay, *The Fractional Fourier Transform with Applications in Optics and Signal Processing*, Wiley, New York, 2001.
- [5] T.M. Lehmann, C. Gonner, K. Spitzer, Survey: interpolation methods in medical image processing, *IEEE Trans. Med. Imaging* 18 (1999) 1049–1075.
- [6] P. Thevenaz, T. Blu, M. Unser, Interpolation revisited [medical images application], *IEEE Trans. Med. Imaging* 19 (2000) 739–758.
- [7] A. Amanatiadis, I. Andreadis, A survey on evaluation methods for image interpolation, *Meas. Sci. Technol.* 20 (2009) 104015.
- [8] H. Shen, X. Li, Q. Cheng, C. Zeng, G. Yang, H. Li, L. Zhang, Missing information reconstruction of remote sensing data: a technical review, *IEEE Geosci. Remote Sens. Mag.* 3 (2015) 61–85.
- [9] A. Papoulis, *Systems and Transformations with Applications in Optics*, McGraw-Hill, Wiley, 1968.
- [10] R. Ranjan, N. Jindal, A. Singh, A sampling theorem for fractional s-transform with error estimation, *Digit. Signal Process.* 93 (2019) 138–150.
- [11] K.B. Wolf, *Geometric Optics on Phase Space*, Springer, 2004.
- [12] J.J. Healy, M.A. Kutay, H.M. Ozaktas, J.T. Sheridan (Eds.), *Linear Canonical Transforms: Theory and Applications*, Springer New York, New York, NY, 2016.
- [13] A. Koç, B. Bartan, H.M. Ozaktas, Discrete linear canonical transform based on hyperdifferential operators, *IEEE Trans. Signal Process.* 67 (2019) 2237–2248.
- [14] Z.-C. Zhang, Uncertainty principle for linear canonical transform using matrix decomposition of absolute spread matrix, *Digit. Signal Process.* 89 (2019) 145–154.
- [15] S. Xu, L. Feng, Y. Chai, B. Du, Y. He, Uncertainty relations for signal concentrations associated with the linear canonical transform, *Digit. Signal Process.* 81 (2018) 100–105.
- [16] X. Huang, L. Zhang, S. Li, Y. Zhao, Radar high speed small target detection based on keystone transform and linear canonical transform, *Digit. Signal Process.* 82 (2018) 203–215.
- [17] Q. Feng, B.-Z. Li, J.-M. Rassias, Weighted Heisenberg-Pauli-Weyl uncertainty principles for the linear canonical transform, *Signal Process.* 165 (2019) 209–221.
- [18] Q. Feng, B.-Z. Li, Convolution and correlation theorems for the two-dimensional linear canonical transform and its applications, *IET Signal Process.* 10 (2016) 125–132.
- [19] F. Zhang, R. Tao, Y. Wang, Discrete linear canonical transform computation by adaptive method, *Opt. Express* 21 (2013) 18138–18151.
- [20] J. Zhao, R. Tao, Y. Wang, Sampling rate conversion for linear canonical transform, *Signal Process.* 88 (2008) 2825–2832.
- [21] E. Meijering, A chronology of interpolation: from ancient astronomy to modern signal and image processing, in: *Proceedings of the IEEE*, vol. 90, pp. 319–342.
- [22] J.A. Parker, R.V. Kenyon, D.E. Troxel, Comparison of interpolating methods for image resampling, *IEEE Trans. Med. Imaging* 2 (1983) 31–39.
- [23] W. Siu, K. Hung, Review of image interpolation and super-resolution, in: *Proceedings of the Asia Pacific Signal and Information Processing Association Annual Summit and Conference*, 2012, pp. 1–10.
- [24] R.W. Schafer, L.R. Rabiner, A digital signal processing approach to interpolation, *Proc. IEEE* 61 (1973) 692–702.
- [25] T. Ramstad, Digital methods for conversion between arbitrary sampling frequencies, *IEEE Trans. Acoust. Speech Signal Process.* 32 (1984) 577–591.
- [26] R.E. Crochiere, L.R. Rabiner, Interpolation and decimation of digital signals: a tutorial review, *Proc. IEEE* 69 (1981) 300–331.
- [27] N.A. Dodgson, Quadratic interpolation for image resampling, *IEEE Trans. Image Process.* 6 (1997) 1322–1326.
- [28] H. Hou, H. Andrews, Cubic splines for image interpolation and digital filtering, *IEEE Trans. Acoust. Speech Signal Process.* 26 (1978) 508–517.
- [29] T. Blu, P. Thevenaz, M. Unser, Linear interpolation revitalized, *IEEE Trans. Image Process.* 13 (2004) 710–719.
- [30] M. Unser, Splines: a perfect fit for signal and image processing, *IEEE Signal Process. Mag.* 16 (1999) 22–38.
- [31] P. Thevenaz, T. Blu, M. Unser, Image interpolation and resampling, in: *Handbook of Medical Imaging, Processing and Analysis*, Academic Press, 2000, pp. 393–420.
- [32] H.C. Andrews, C.L. Patterson, Digital interpolation of discrete images, *IEEE Trans. Comput.* C-25 (1976) 196–202.
- [33] S.C. Pei, Y. Lai, Signal scaling by centered discrete dilated Hermite functions, *IEEE Trans. Signal Process.* 60 (2012) 498–503.
- [34] S.C. Pei, J.J. Ding, W.L. Hsue, K.W. Chang, Generalized commuting matrices and their eigenvectors for DFTs, offset DFTs, and other periodic operations, *IEEE Trans. Signal Process.* 56 (2008) 3891–3904.
- [35] D.H. Mugler, S. Clary, Y. Wu, Discrete Hermite expansion of digital signals: Applications to ECG signals, in: *Proceedings of the DSP Workshop of IEEE Signal Process. Soc.*, 2002, pp. 262–267.
- [36] K.B. Wolf, *Integral Transforms in Science and Engineering (Chapter 9: Construction and properties of canonical transforms)*, Plenum Press, New York, 1979.
- [37] H.M. Ozaktas, M.A. Kutay, C. Candan, *Transforms and Applications Handbook*, CRC Press, Boca Raton, New York, NY, 2010, pp. 14–1–14–28.
- [38] A. Koç, Operator theory-based discrete fractional Fourier transform, *Signal Image Video Process.* 13 (2019) 1461–1468.
- [39] K. Yosida, *Operational Calculus: A Theory of Hyperfunctions*, Springer, New York, USA, 1984.
- [40] A. Koç, H.M. Ozaktas, Operator theory-based computation of linear canonical transforms, in preparation (2020).
- [41] M. Nazarathy, J. Shamir, Fourier optics described by operator algebra, *J. Opt. Soc. Am.* 70 (1980) 150–159.

Aykut Koç is a Research Assistant Professor in Electrical and Electronics Engineering Department and in the National Magnetic Resonance Research Center (UMRAM) at Bilkent University, Ankara, Turkey. He received the B.S. degree in Electrical and Electronics Engineering from Bilkent University, Ankara, Turkey, in 2005, the M.S. degree in electrical engineering in 2007, the M.S. degree in management science and engineering in 2009, and the Ph.D. degree in electrical engineering in 2011, all from Stanford University, Stanford, CA. He taught part-time in the Department of Electrical and Electronics Engineering, Middle East Technical University (METU). He is a Senior Member of IEEE. He has authored or co-authored around 46 research papers, 1 book chapter and 4 patents (1 issued, 3 pending). His current research interests are in natural language processing and signal/image processing.

Burak Bartan received the B.S. degree in Electrical and Electronics Engineering from Bilkent University, Ankara, Turkey, in 2016. He is currently working toward the Ph.D. degree in Electrical Engineering, Stanford University, CA, USA. During his undergraduate studies with Bilkent University, he worked on applying fractional Fourier, and linear canonical transforms to image compression and discrete linear canonical transforms. His academic interests include large-scale computation, machine learning, optimization and signal processing.

Haldun M. Ozaktas received the B.S. degree from Middle East Technical University, Ankara, Turkey, in 1987 and the Ph.D. degree from Stanford University, Stanford, CA, USA, in 1991. In 1991, he joined Bilkent University, Ankara, Turkey, where he is currently a Professor of electrical engineering.

In 1992, he was with the University of Erlangen-Nurnberg, Bavaria as an Alexander von Humboldt Foundation Postdoctoral Fellow. During the summer of 1994, he worked as a Consultant with Bell Laboratories, Holmdel, NJ, USA. He has authored of about 120 refereed journal articles, 20 book chapters, and 120 conference presentations and papers, more than 40 of which have been invited. He has also authored of the book *The Fractional Fourier Transform* (Wiley, 2001) and edited the books *Three-Dimensional Television* (Springer, 2008) and *Linear Canonical Transforms* (Springer, 2016). His academic interests include signal and image processing, optical information processing, and optoelectronic and optically interconnected computing systems. He has a total of more than 6000 citations to his work recorded in the Science Citation Index (ISI). He is the recipient of the 1998 ICO International Prize in Optics and one of the youngest recipients ever of the Scientific and Technical Research Council of Turkey (TUBITAK) Science Award (1999), among other awards and prizes.

He is also one of the youngest-elected members of the Turkish Academy of Sciences and a Fellow of the IEEE, OSA and SPIE.